Complex structure / composition relationship in thin films of AlCoCrCuFeNi high entropy alloy

Vincent Dolique, Anne-Lise Thomann, Pascal Brault, Yves Tessier, Pascale Gillon

Complex structure / composition relationship in thin films of AlCoCrCuFeNi high entropy alloy

V. Dolique[1], A-L. Thomann[1], P. Brault[1], Y. Tessier[1], P. Gillon [2]

[1]Groupe de Recherche sur l'Energétique des Milieux Ionisés,

UMR 6606 CNRS-Université d'Orléans BP 6744, 45067 Orléans Cedex 2, France.

[2] ICARE CNRS 1C Av. de la Recherche Scientifique, 45071 Orléans Cedex 2, France.

E-mail : vincent.dolique@univ-orleans.fr, anne-lise.thomann@univ-orleans.fr.

Abstract

We have studied the deposition of AlCoCrCuFeNi high entropy alloy (HEA) thin films on Si (100) substrates by DC magnetron sputtering process. Three mosaic targets have been used for easily tailoring the film composition. Energy dispersive X-ray spectrometry analysis has shown that chemical composition can be modified around the nominal value by tuning the ratio of the powers applied to the magnetron targets. The deposition rate is directly related to the power sum. Moreover, various surface morphologies have been evidenced by scanning electron microscopy and correlated to the crystalline phases present in the films. Morphology and crystalline structure have been found to depend on the chemical composition. Wetting contact angle has been measured with water droplets, showing that the hydrophobic properties of the thin films depend on their characteristics.

Keywords: Alloys; Thin films; Plasma sputtering deposition; Anti-adhesive properties

1. Introduction

High Entropy Alloys (HEA) are metallic compounds containing six to thirteen metallic elements in equimolar ratios. If thirteen elements are arbitrary selected, then a theoretical value of 7099 alloys are able to be synthesized, and even more, if some elements such as C or B are added in low concentration. For example, works have been done on AlCoCrCuFeNi, $AlCo_{0.5}CrCuFe_{1.5}Ni_{1.2}$ or $AlCo_{0.5}CrCuFe_{1.5}Ni_{1.2}B_{0.1}C_{0.15,}$ AlMoNbSiTaTiVZr, AlFeTiCrZnCu [1-3]. Because HEA are composed of more than six elements, their mixing entropy is high, leading to the formation of random solid solutions during solidification, rather than inter-metallic compounds [1]. To estimate the entropy of metallic alloy formation, Boltzmann's hypothesis can be made [4] and the following equation can be used:

$$\Delta S = -R\ln\left(\frac{1}{n}\right) = R\ln(n)$$

where R is the ideal gas constant and *n* the number of mixed elements. From n=6, ΔS becomes higher than the mixing entropy of most intermetallic compounds [4], which leads to the preferential formation of solid solutions. From n=5 to n=13 elements, alloys have entropy between 1.61R and 2.56R and belong to the High Entropy domain, as defined by J.W. Yeh [1]. The limit of thirteen elements is arbitrary. Beyond this value, it has been shown that the benefit brought by adding more elements would be small.

In these alloys, complex micro-structures are thus avoided and sluggish diffusion leads to the formation of amorphous or nanocrystallized (FCC and/or BCC phases) structures [1]. They exhibit very interesting properties: hydrophobicity, high stiffness, strength and toughness, high hardness and good temperature stability, improved corrosion resistance, superplasticity and high-strain-rate superplasticity. They are environmentally friendly: recyclable, lead-free, cadmium-free, and even if they contain Cr, the toxic Cr^{6+} specie is never formed [1].

History of HEAs is relatively recent and has principally been written by J-W Yeh and al. [5-12]. To synthesize bulk pieces or thick films of HEA, they employ arc melting process [5-8] and many techniques such as rapid solidification, thermal spray forming or mechanical alloying [1]. Only few studies on HEA thin films have been published [5, 9-12] and they all deal with the sputtering of an alloyed target formed by melting or casting. In this article, we use magnetron sputtering of mosaic targets composed of pure elements [13] to deposit HEA thin films. This deposition technique has many advantages: 1) control of the film thickness in a wide range (in our study between 300 nm to 2 μm), 2) variation of the stoechiometry by

adjusting the target powers, 3) introduction of a concentration gradient for one or more elements. Concentration gradients along the film thickness can be useful to improve adherence of thin film on the substrate, preserving the interesting properties of HEA at the outer surface.

To deposit thin films of AlCoCrCuFeNi, three mosaic targets are used. Various stoechiometries near the theoretical one (exact equimolar ratios: AlCoCrCuFeNi) are studied. Crystalline structure of HEA thin films are analyzed by X-Ray Diffraction (XRD). To observe the morphology and study the composition, we use Scanning Electron Microscopy (SEM) coupled with Energy Dispersive X-ray Spectrometry (EDS). One of the interesting properties of the HEA is their anti-adhesion, which makes them an alternative candidate to Teflon (containing fluorine) in many applications such as food industry, packaging, cosmetic… In order to evaluate the anti-adhesive properties of the thin films, wetting contact angle measurements are performed.

2. Experimental procedure

A detailed description of the experimental device is given by P. Plantin et al. [14]. Briefly, three magnetron targets are focused onto rotating Si (100) substrates. The six chemical elements are arranged on the targets (Fig. 1): Fe, Co and Ni are on target 1, Cu and Cr on target 2 and Al on target 3. This distribution has been chosen for the following reasons. Al sputtering yield being the lowest, a large area, corresponding to the size of a whole target, is necessary to reach the required ratio. The presence of a single magnetic element in a target would have led to local perturbation of the permanent magnetic field. To avoid this phenomenon, we have chosen to build a target with the three magnetic elements: Fe, Co and Ni. To ensure an efficient sputtering process of this target, a thin thickness (1 mm) is required. Finally, the last target is composed of the remaining elements: Cr and Cu.

The following equation has been used to calculate the relative exposed area A_i of each element and to obtain the equimolar stoechiometry AlCoCrCuFeNi:

$$X_i = \frac{Y_i \times A_i \times 100}{\sum Y_i \times A_i}$$

Where, Y_i is the sputtering yield, A_i the surface area and X_i the percentage of element i.

The X_i value required to obtain an equimolar alloy with six elements is 16.7 %. The power (on each target) is varied to achieve composition near the equimolar one. The same argon

pressure is used (1 Pa) during deposition runs, that are performed without heating of the substrate. The substrate temperature remains floating and stays below 100°C. The targets-to-substrate distance is kept constant, equal to 90 mm.

The characteristics of the HEA thin films are examined with scanning electron microscopy (Hitachi S4200) equipped with EDS (Oxford) at the CME (Centre de Microscopie Electronique) of the University of Orleans. SEM observations are performed in both plane and cross-section views to investigate the surface morphology, thickness and structure of the film. EDS analysis, allows to evaluate the chemical composition. XRD measurements are carried out in a conventional Bragg–Brentano θ-2θ geometry with the Cu *K*α radiation (Philips X'Pert Pro). The wetting contact angle technique is used to determinate the contact angle (θ) between the film surface and water. These data give some insights into the anti-adhesive properties of the alloys. Before measurements, the film surface is cleaned with alcohol and acetone. A small droplet of distilled water (10 µl) is put onto the surface. Some experiences have been performed three times to check the reproducibility of measurements. A photo of the cross section is taken to measure the contact angle. If $\theta > 90°$, the alloy is non-wetting, it is hydrophobic. For $\theta < 90°$, the alloy is hydrophilic [15].

3. Results and discussion

Twelve thin films have been synthesized with different powers applied to the targets. The deposition rate measured from SEM cross sections is given in Fig. 2 versus the power sum. The observed linear dependence was expected, since the mass ejected from the three targets rises with the power. Deposition rates are similar to what is usually found in magnetron sputtering processes [16]. This deposition technique allows to accurately control the thickness of the thin films in a large range: from 10 nm to several µm. In the present deposition conditions, for 5 to 25 minutes deposition times, the thickness varies from 0.3 to 1.8 µm, with deposition rates from 35 nm/min to 95 nm/min.

Morphology and structure

Plane view (Fig. 3) and cross section (Fig. 4) SEM observations have been carried out for showing surface morphology and for providing some insight into the growth mode. Three typical thin film morphologies (A, B and C) have been identified. Table 1 gives the micro-

structure of the twelve films. Structure A is composed of grains of 100 nm with sharp shape. In structure B, round grains of 10 nm are present, and structure C exhibits grains of 100 nm, subdivided in lamellar grains of 10-20 nm. From cross sections it is shown that in structure A, the growth begins with thin dense columns, which broaden out to give rise to sharp heads. The broadening effect is less visible in structure B, columns remaining relatively cylindrical and thin along the thickness. The section is dense, and the surface seems to be smoother. In structure C, the columns broaden out like in A, the sharp tips at the top are also observed, but the columns are porous, exhibiting flake structure. This leads to the appearance of subdivided sharp edge grains at the surface. The three surface morphologies that have been evidenced are thus linked to the growth mode of the base columns. These structures are typical of deposition by magnetron sputtering process [17].

From XRD analysis three crystalline structures have been evidenced: BCC solid solution, FCC solid solution and amorphous (or nanocrystalline) phases. These phases have already been observed for bulk alloy by J.W. Yeh *et al* [5, 8] for cast ingots or thin films deposited by sputtering of targets made of the ingots. It has been shown that the BCC and FCC lattice parameters are shifted compared to pure element phases because of distortions induced by the stacking of atoms with different sizes. The correlation between the morphologies of the films (SEM images), which depends on the growth mode, and the observed crystalline phases is clearly observable. This is illustrated in Fig. 5 where the corresponding diffraction spectra are given for A, B and C structures. The formation of sharp edge 100 nm grains (structure A) is associated to the presence of the BCC phase, whereas the small round grains of structure B correspond to the FCC phase presence. It is interesting to note that on structure C films, no diffraction peaks are detected, which could be attributed to amorphous or nanocrystalline phases. The morphology observed by SEM indicates that the lack of diffraction peaks is rather due to the presence of small grains. Indeed, in structure C, sharp edge grains of about 100 nm are subdivided into fine lamellar grains, as shown in the insert of Fig. 3.

It should be noted that mixing of BCC and FCC phases have not been obtained in the present study, whereas mixed structures are often found in bulk samples. In these cases, inter-dendrite and dendrite zones are evidenced, characteristic of the synthesis by these techniques. They are several μm large and exhibit small variation of composition and crystalline structure. Such heterogeneities are not found on HEA thin films obtained in the present work; the composition of a single grain being the mean composition of the alloy. This is due to the deposition technique used. Because of the magnetron arrangement, the fluxes of the six elements closely overlap onto the substrate surface. Moreover, it seems that surface migration

that might lead to composition and structure inhomogeneity, is negligible due to the rapid formation of the alloy, the substrate not being heated. Deposition by magnetron co-sputtering is thus found to promote chemical mixing and to hinder atomic diffusion through the film.

Role of the deposition parameters

It is known that the crystalline structure of bulk HEAs synthesized by melting depends on the chemical composition and the processing route [1]. To our knowledge, no study has been published on the formation of these structures for HEA thin films. In the following we will try to evidence what is driving the structure growth of HEA films.

From SEM observations, it is shown that the crystalline structure of the HEA deposits, which is correlated to the morphology, depends on the growth mode. In plasma sputtering deposition, the parameters that may influence the growth mode are the flux and kinetic energy of the depositing atoms and the flux and kinetic energy of the energetic plasma species interacting with the substrate during the growth. The surface temperature can also play a role. In our case, it remains below 100°C.

In the present study, only the powers of the three targets are varied, corresponding to target voltages in the range 200V to 500V, voltage which determines the argon ion sputtering energy (accelerating voltage minus plasma potential). Calculations show that, in our experimental conditions the kinetic energy of the depositing metallic atoms does not depend on the argon ion sputtering energy but rather on the argon pressure and the target to substrate distance, that have not being modified [18]. The kinetic energy of the metal atoms is thus constant and can be not responsible for the change of morphology. Moreover, the substrate being located far away from the targets, there is no interaction with the sputtering plasma and thus, a modification of the energetic level of the Ar plasma (kinetic energy and flux of energetic species) will not influence the deposition process. The last deposition parameter that must be discussed is the total atom flux, i.e. the deposition rate, which is related to the target powers (see Fig. 2). In Table 2 the applied powers are given for the twelve deposits as well as the corresponding structure observed by SEM. No clear correlation can be found between the total power (or the deposition rate) and structure. This again shows that the deposition parameters are not driving the growth mode of the films.

Structure/composition relationship

The only difference between deposits is the chemical composition (correlated to the target power ratios). The stœchiometry of the thin films determined by EDS is sorted into structure

in the plot of Fig. 6. The dotted horizontal line corresponds to the theoretical composition for an equimolar HEA of six elements. If the percentage of one of the elements stays above 35%, the alloy is no more considered as a HEA. In this case, one of the elements being principal, the alloy composition is closer to the definition of a metallic glass [19, 20]. It can be seen in Fig.6 that this is the case of several deposits (A17a, C25a…). Moreover, the required composition (16.7% for each element) is never reached. The fraction of an element is found to be proportional to the ratio between the power applied to its target and the power sum. Consequently, it is possible from empirical laws to synthesize a HEA film with a desired composition. Nevertheless, the range of accessible stoechiometries is limited by the fact that several elements belong to the same target. To extend the composition domain, the mosaic targets should be modified.

From the literature on bulk HEAs, it appears that a complex relationship exists between crystalline structure and composition. For instance, the presence of copper, which crystallizes into a FCC structure, is found to promote the formation of a FCC solid solution [8]. This is also the case for Co and Ni, whereas, Cr and Fe, crystallizing into BCC structure, induce the formation of a BCC solid solution [1]. However, pure Al having also a FCC structure, leads to the formation of a FCC solid solution. Yeh *et al* have even shown that for Al atomic percentages higher than about 15 %, the BCC structure is stabilized [5]. This particular behavior of aluminum is attributed to its special electronic structure, metallic or non-metallic, depending on its surroundings [4].

From Fig. 6 general trends for the formation of FCC, BCC or amorphous structures can be discussed. Structure A is obtained for films containing high concentrations of Cr and/or Al, which is in agreement with BCC solid solution formation as explained above. In structure A (Fig. 5), the α (110) reflection stands at $2\theta=44.9°$, which is +0.7° shifted from pure Cr (110) peak given at $2\theta=44.2°$. Except for Al atom, Co, Cu, Fe and Ni have smaller atomic radius than Cr one (see Table 3). Thus, the shift of the peak position versus high angle values can be attributed to the substitution of Cr by these atoms in the BCC structure, which leads to a decrease of the lattice parameter. Formation of structure B corresponds to thin films with the less dispersed atomic percentages, i.e. composition the closest to the equimolar repartition. Calculating the atomic percent of FCC stabilizing elements (Cu, Co and Ni), it is found that films of the B family have the highest values of all the films (more than 50%) and exhibit the lowest Al concentrations (less than 15 %). Both trends lead to the stabilization of FCC solid solution. Ni being the more abundant element, it is interesting to compare its β (111)

reflection with the HEA one. A negative shift of 0.6° exists between pure Ni value (44.5°) and the HEA peak at 43.9° (Fig.5). Again, taking the structure of pure Ni as reference, the substitution by larger atoms (see Table 3) would lead to an increase of the lattice parameter and thus to a shift of the β (111) peak position to lower values. Finding a composition consistency is less easy in the case of C structure. Especially for C25a and C25b samples that are very close to A17a and A19a respectively. It seems that a tiny variation of the percentage of one element can induce a structure shift from a solid solution to a disordered state (Fig. 5). Nevertheless, it should be noted that all HEA films with C structure have very low Cu amounts (less than 10%). Since copper has been found to play a major role in the stabilization of crystalline phases [5], this feature might be an important point.

Wetting properties

Preliminary results of wettability property study are given in Fig.7 showing pictures of a distilled water droplet deposited onto HEA films (structures A, B or C) and on three reference materials: stainless steel, brass and Teflon. Teflon is analyzed since it is widely used at present for its very good hydrophobic property. Stainless steel and brass are tested for comparison because they are commonly used in industry. Advancing angle measurements are shown in Table 4. For Teflon, a contact angle of 104° is found in good agreement with values from literature [21]. The lowest contact angles are measured for stainless steel and brass alloys, respectively 65° and 73°. A24b and B24c exhibit high contact angles (109° and 101°), showing that both films are hydrophobic. An intermediate contact angle (83°) is measured for C25a. As $\theta < 90°$, this alloy is considered as slightly hydrophilic.

It is interesting to note that a difference of wetability is obtained between structure A, B and C. Hydrophobicity is known to depend both on morphology and chemical composition. For example, M.J. Rizvi et al. [22] have observed such a dependence on Sn–0.7Cu and Sn–0.7Cu–0.3Ni. A concentration of 0.3% of Ni improves the hydrophilicity of thin films. T. Berlind et al. [23] have observed the effect of concentration of Si on the hydrophilicity of Si-C-N alloy. They conclude on the dependence of the thin films hydrophilicity on the chemical composition.

In the present study, we have evidenced that the HEA thin film structure is correlated to a chemical composition family. Both features are thus linked. From contact angle measurements, it can be concluded that formation of BCC or FCC solid solutions, corresponding to high Cr and Al, or high Ni (and FCC stabilizing elements) concentrations respectively, enhances the anti-adhesive property of the films. When the lattice distortion

induced by the presence of 6 elements of different sizes is too large and leads to a disordered state (structure C), the hydrophobic feature is less pronounced.

4. Conclusion

In this study AlCoCrCuFeNi HEA thin films have been successfully deposited by magnetron co-sputtering of three mosaic targets. Relatively high deposition rates have been measured. By tuning with the target powers, chemical composition of the films has been varied in a range close to the equimolar one, the other deposition parameters remaining constant. This has allowed to study the influence of the chemical composition on the thin films characteristics. Indeed, compared to deposition performed from sputtering of alloy targets, variation of the element concentrations can be easily done by adjusting the target powers.

Three film families have been evidenced exhibiting three surface morphologies and crystalline structures: BCC, FCC solid solutions and a disordered state. The relationship between composition and structure has been discussed, and general trends have been drawn in good agreement with bulk HEAs. BCC structure seems to be stabilized by the presence of Cr and Al in higher concentrations than the other elements. Low Al contents associated with high Cu, Co and Ni concentrations promote the formation of FCC solid solution. However, it appears that very small variations of the chemical composition can induce lattice distortion and leads to a disordered state, which make difficult anticipation of the structure from the deposition parameters. This confirms that the relationship between structure and composition is complex as proved by Yeh et al that has reported two different crystalline structures for a bulk HEA synthesized in the same experimental conditions [9, 25].

Contact angle measurements conducted with water droplets have been performed to characterize the anti-adhesive property of the films. It is shown that thin films with FCC or BCC solid solutions are highly hydrophobic, with values close to Teflon one, whereas a disorder state (associated to a composition family) exhibits a less hydrophobic feature. These results are very promising for future substitution of Teflon for HEAs.

References :

[1] J-W Yeh et al., Ann. Chim. Sci. Mat. 31(6) (2006) 663.

[2] M.-H. Tsai, J.-W. Yeh, J.-Y. Gan, Thin Solid Films 516 (2008) 5527.

[3] S. Varalakshmi, M. Kamaraj, B.S. Murty, Journal of Alloys and Compounds 460 (2008) 253.

[4] C. Li, J.C. Li, M. Zhao, Q. Jiang, Journal of Alloys and Compounds (2008), doi:10.1016/j.jallcom.2008.07.124 (in press).

[5] J-W Yeh et al., Advanced Engineering Materials 6 (2004) 299.

[6] U.S. Hsu, U.D. Hung, J.W. Yeh, S.K. Chen, Y.S. Huang and C.C. Yang, Materials Science and Engineering: A 460-461 (2007) 403.

[7] J.-W. Yeh, S.-Y. Chang, Y.-D. Hong, S.-K. Chen and S.-J. Lin, Materials Chemistry and Physics 103 (2007) 41.

[8] C.-C. Tung, J.-W. Yeh, T.-T. Shun, S.-K. Chen, Y.-S. Huang and H.-C. Chen, Materials Letters 61 (2007) 1.

[9] H.-W. Chang, P.-K. Huang, J.-W. Yeh, A. Davison, C.-H. Tsau and C.-C. Yang, Surface and Coatings Technology 202 (2008) 3360.

[10] M-H Tsai, Ji-W Yeh and J-Y Gan, Thin Solid Films 516 (2008) 5527.

[11] T-K Chen, M-S Wong, T-T Shun and J-W Yeh, Surface and Coatings Technology 200 (2005) 1361.

[12] T.K. Chen, T.T. Shun, J.W. Yeh and M.S. Wong, Surface and Coatings Technology 188-189 (2004) 193.

[13] Patent N° WO/2008/028981

[14] P. Plantin, A.-L. Thomann, P. Brault, P.-O. Renault, S. Laaroussi, P. Goudeau, B. Boubeker, T. Sauvage, Surface and Coatings Technology 201 (2007) 7115.

[15] Y. Sutjiadi-Sia, P. Jaeger, R. Eggers, Journal of Colloid and Interface Science 320 (2008) 268.

[16] Messier R and Yehoda J E J. Appl. Phys. 58 (1985) 3739.

[17] Dirks A G, Wolters R A and De Veirman A E M, Thin Solid Films 208 (1992) 181.

[18] P. Brault, A.L. Thomann, J.P. Rozenbaum, C. Andreazza, P. Andreazza, B. Rousseau, H. Estrade-Szwarckopf, G. Blondiaux, T. Sauvage, Y. Tessier, A. Berthet, J.C. Bertolini, F.J. Cadete Santos Aires, F. Monnet, C. Mirodatos, C. Charles, R. Boswell, Recent Res. Devel. Vacuum Sci. & Tech. 2 (2000) 35.

[19] T. Zhang, A. Inoue and T. Masumoto, Mater. Trans. JIM 32 (1991) 1005.

[20] Z.P. Lu, C.T. Liu, Acta Materia 50 (2002) 3501.

[21] Dupont de Nemours and company, Fluoroproducts, J.R Fleming and al.

[22] M.J. Rizvi , C. Bailey, Y.C. Chan, H. Lu, Journal of Alloys and Compounds 438 (2007) 116.

[23] T. Berlind, N. Hellgren, M. P. Johansson, L. Hultman, Surface and Coatings Technology 141(2001)145.

[24] J.-M. Wu and al., Wear 261 (2006) 513.

Table Captions

Table1. Classification of the thin films depending on their surface morphology.

Table2. Power on the three targets and power sum during the twelve deposition runs.

Table 3. Crystal structure and atomic radii (from reference 6) of Al, Co, Cr, Cu, Fe and Ni elements.

Table 4. Contact angle measurements.

Table 1

Structure A Sharp edge grains	**Structure B** round grains	**Structure C** subdivided sharp edge grains
A24b	B24c	C25a
A23a	B20a	C23b
A24a	B18a	C25b
A17a		C27a
A19a		

Table 2

Name	Power on target 1 (W)	Power on target 2 (W)	Power on target 3 (W)	Total Power (W)	Type of structure	Thickness (nm)
A24b	180	100	21	301	A	890
C23b	110	180	27	317	C	975
A23a	190	170	18	378	A	1080
B20a	180	280	30	490	B	290
A24a	300	180	12	492	A	1315
B24c	180	310	15	505	B	1410
B18a	180	310	30	520	B	340
C27a	180	310	147	637	C	1745
C25a	180	160	362	702	C	1830
C25b	180	160	501	841	C	925
A17a	190	170	500	860	A	475
A19a	280	170	500	950	A	620

Table 3

Name of elements	Al	Cr	Fe	Co	Ni	Cu
Crystal structure	FCC	BCC	BCC	HCP	FCC	FCC
Atomic radius (Å)	1.582	1.423	1.411	1.385	1.377	1.413

Table 4

	Stainless Steel	Brass	Teflon	A24b	B24c	C25a
Contact angle measurement θ (deg)	65	73	104	109	101	83

Figure 1

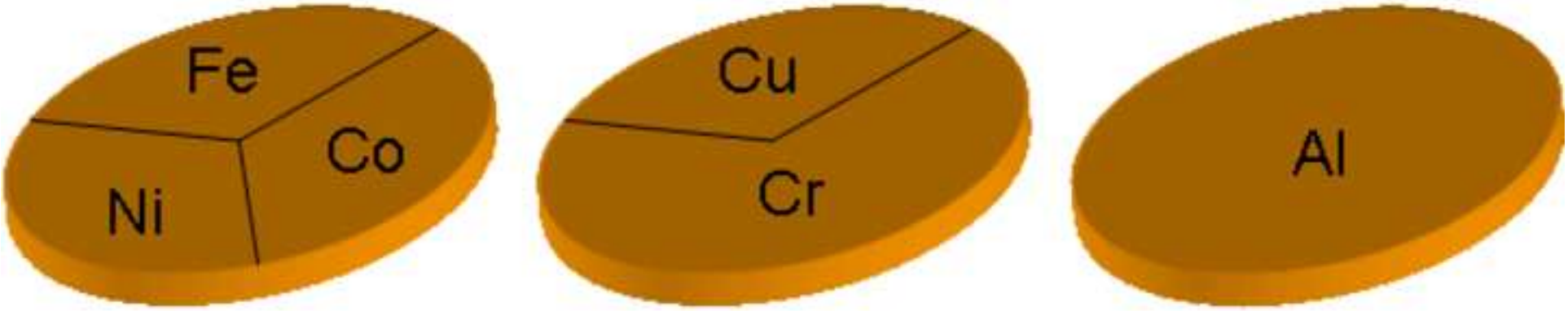

Target 1 Target 2 Target 3

Figure 2

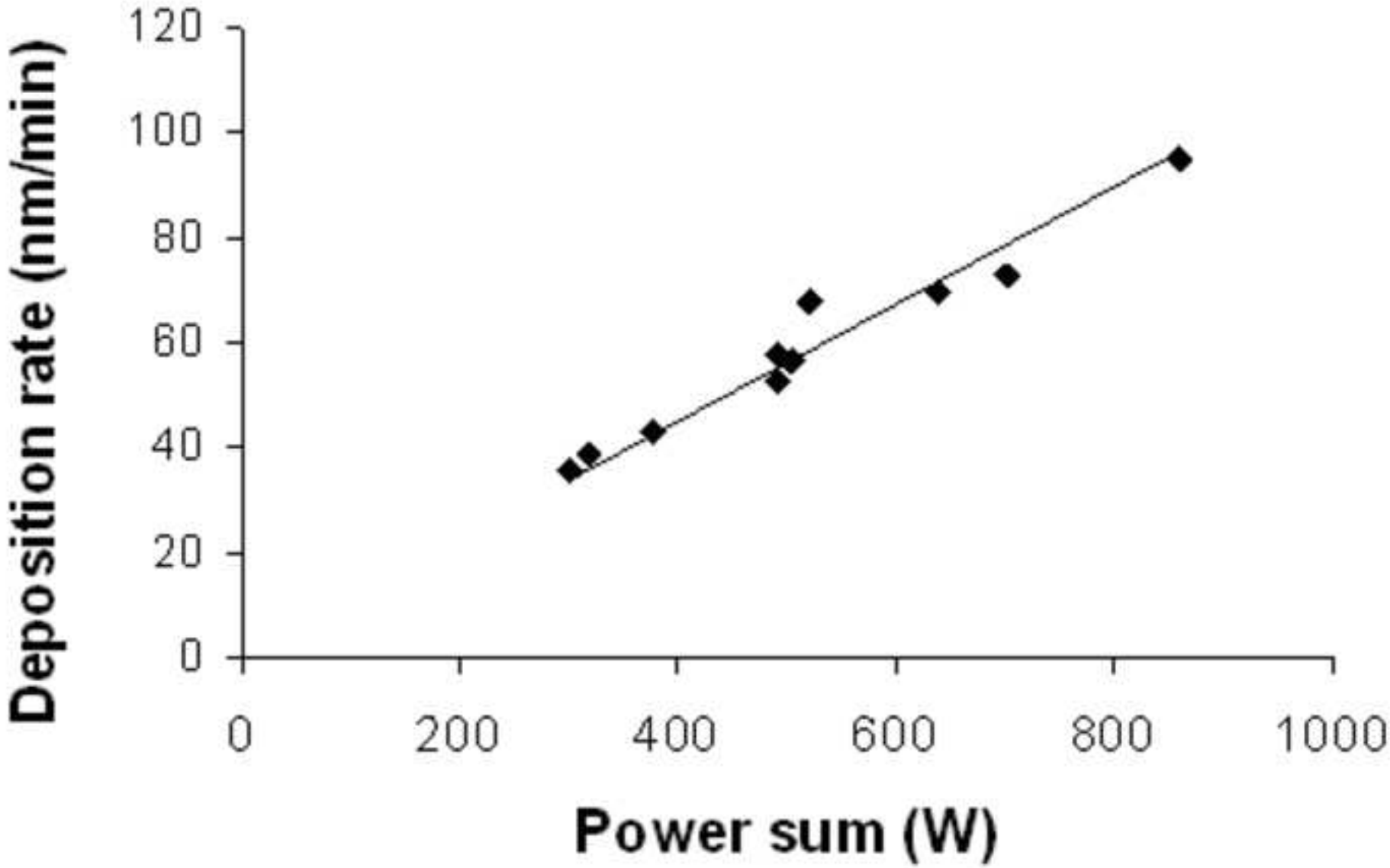
Deposition rate (nm/min)
120
100
80
60
40
20
0
0
200
400
600
800
1000
Power sum (W)

Figure 3

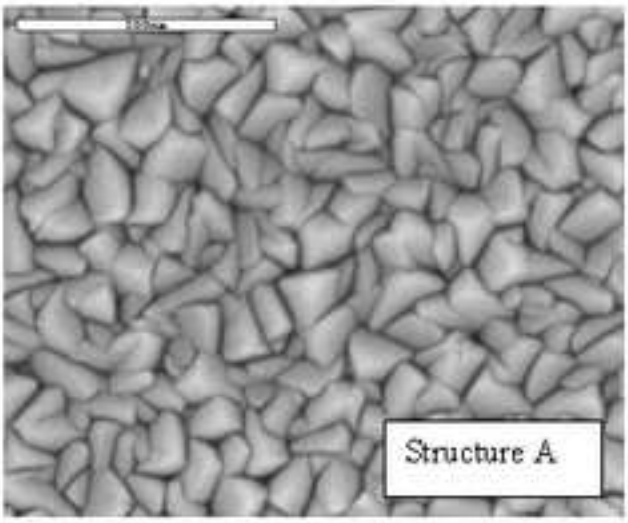

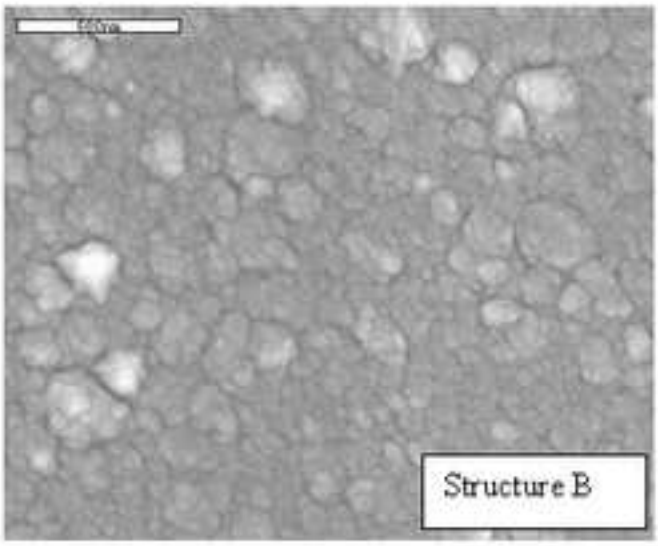

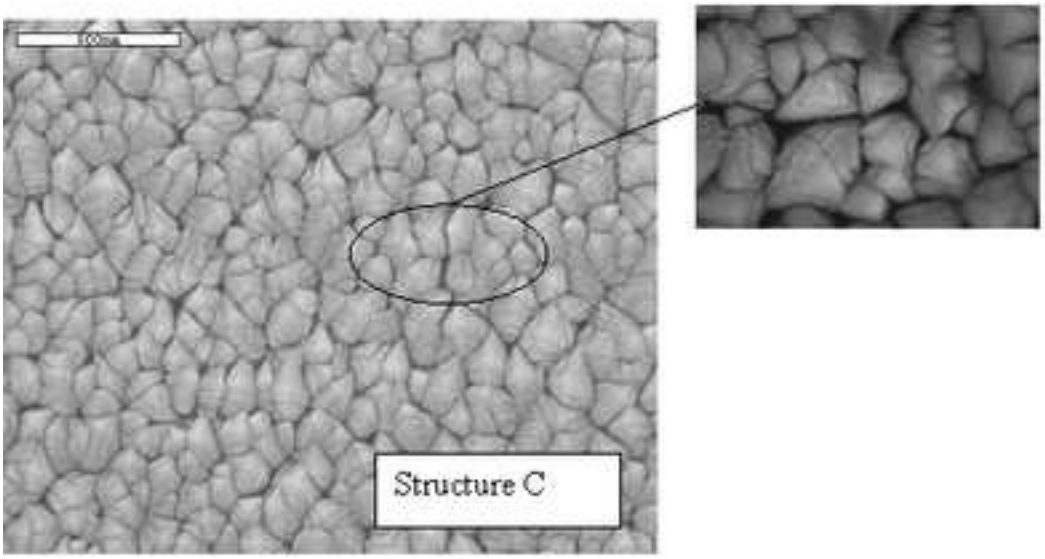

Figure 4

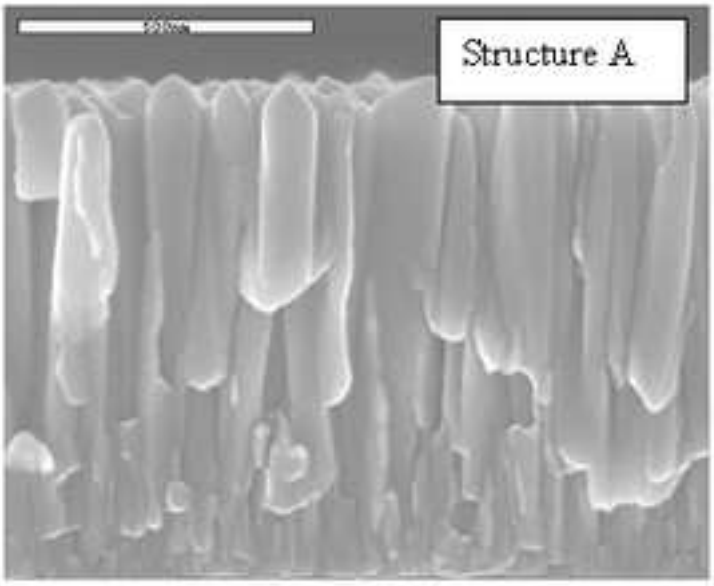

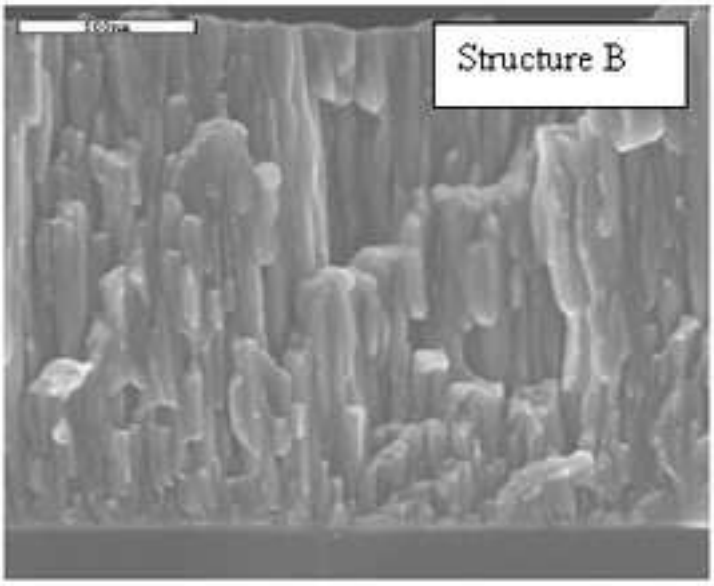

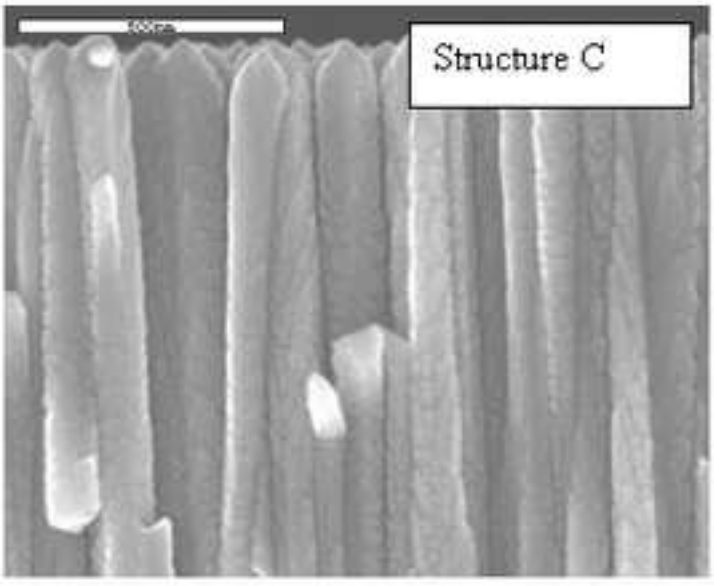

Figure 5

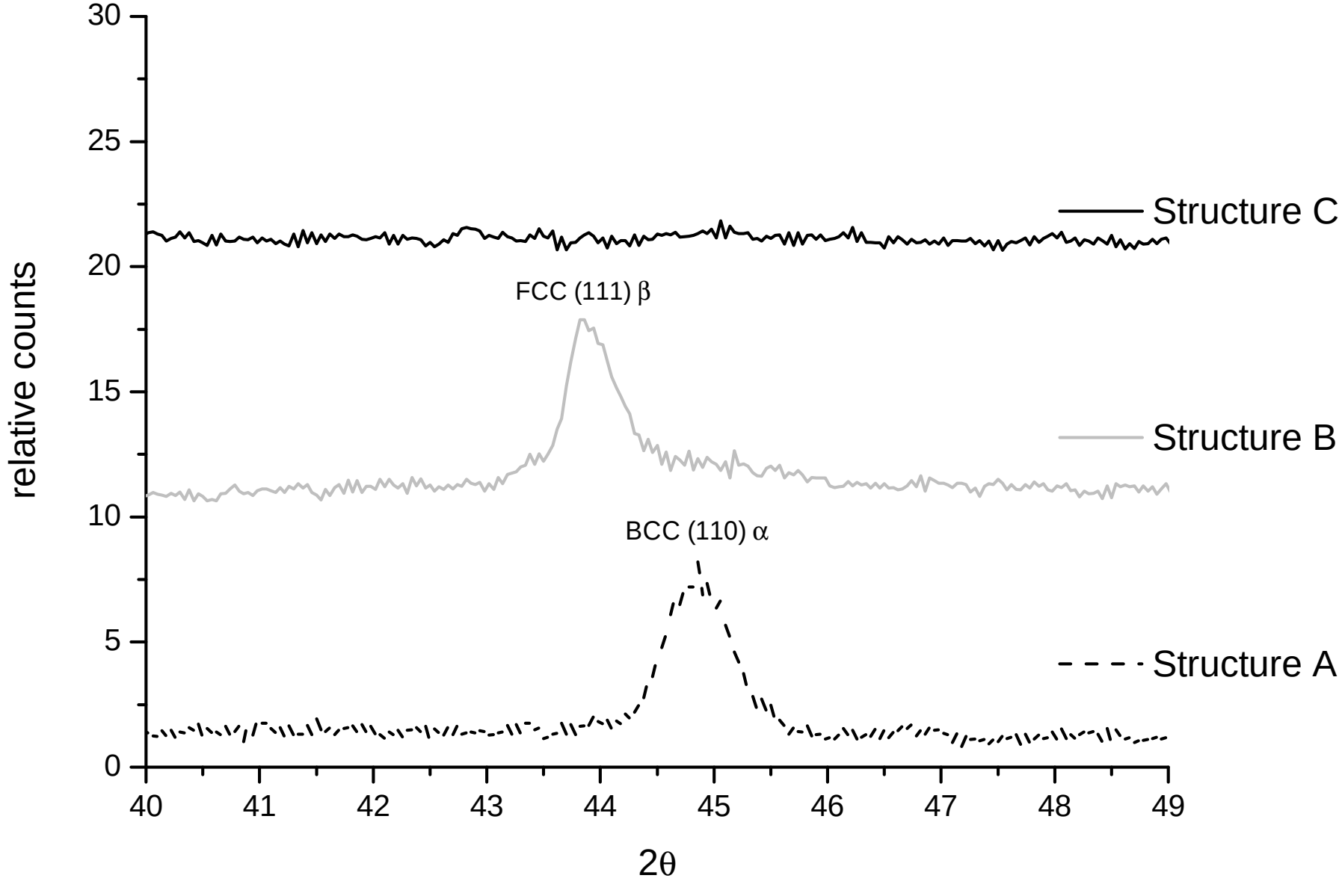
30
25
20
15
10
5
0
relative counts
40
41
42
43
44
45
46
47
48
49
2θ
FCC (111) β
BCC (110) α
Structure C
Structure B
Structure A

Figure 6

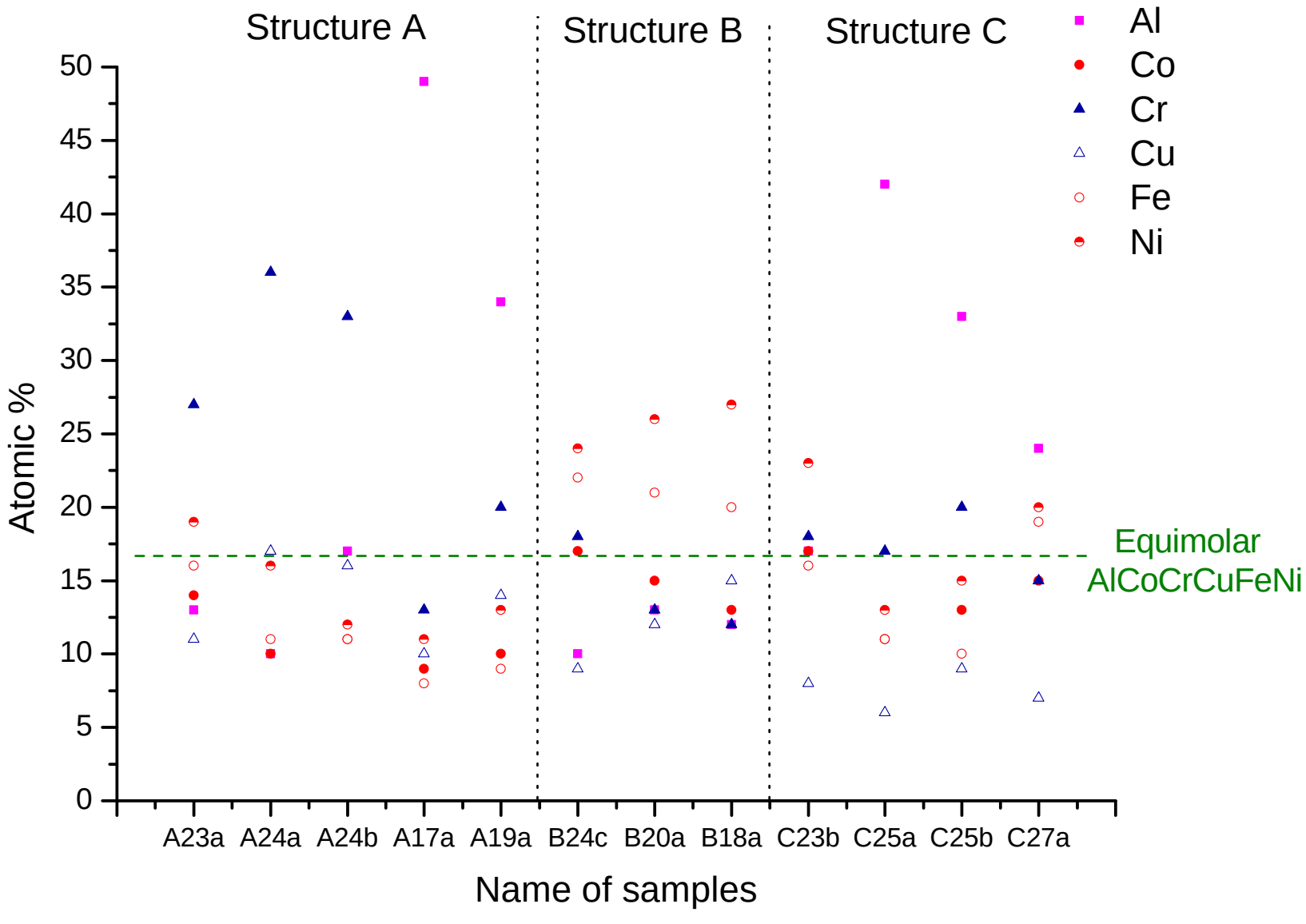
Structure A
Structure B
Structure C
Al
Co
Cr
Cu
Fe
Ni
Equimolar
AlCoCrCuFeNi
Atomic %
0
5
10
15
20
25
30
35
40
45
50
A23a
A24a
A24b
A17a
A19a
B24c
B20a
B18a
C23b
C25a
C25b
C27a
Name of samples

Figure 7

Stainless Steel

Brass

Teflon

A24b

B24c

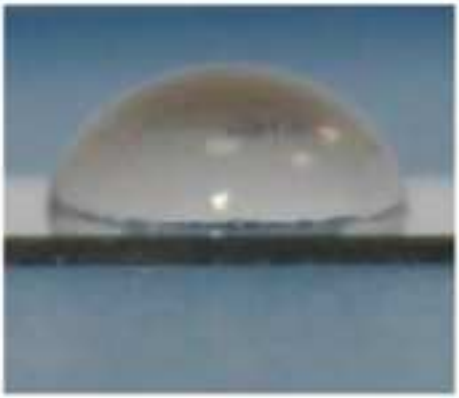

C25a